國立交通大學
物理研究所
碩士論文

量子環的 Aharonov-Bohm 效應

研 究 生 ： 陳光胤

指導教授 ： 褚德三

中華民國九十五年六月

獻給 我摯愛的父母

謝 誌

時光荏苒，碩士班兩年竟如此匆匆，回憶人生至此，在交大物理所的兩年無庸置疑，是我最黃金的時刻，不管在智識上，品德上，都有長足的進步。感謝爸媽一路上的支持，在各方面都給予我最大的空間，讓我可以心無旁騖的專心工作。感謝褚德三教授和陳岳男博士，和你們相處討論和作研究，實在是如沐春風，褚老師的身教言教，豁達的人生觀和對物理的喜愛，在在影響了我許多，岳男慈濟人和氣的個性和對問題認真的態度，也讓我在踏上研究路途的開始，不怕挫折而且有很好的訓練。感謝林高進博士、官文絢博士、邱裕煌學長、廖英彥學長、吳互榮，常與我討論提供意見，感謝李宗上教授、唐英瓚學長在程式上的提點和資料上的幫忙，感謝李哲明學長，總是和氣的聽我對理論提出天馬行空的胡思亂想。感謝負責實驗部分的周武清教授、楊祝壽博士、院繼祖學長、周瑞雯學姊，謝謝你們常常提供我實驗上的知識，使我的想法不至閉門造車，也更能了解實際實驗上的量測。感謝張正宏教授，您是個良師，更是個益友。感謝江進福教授在口試時給予許多寶貴的意見。感謝物理所的夥伴們：旭庭、瑞仁、祥瑞、德明、政展、奎霖、學弟勤倫、平翰、孟聰，與我常常的討論或聊天遊玩，謝謝你們大家！ 這是我研究生涯的開始，很感謝有你們大家的支持和鼓勵，讓我有信心繼續往學術這條路邁進。

量子環的 Aharonov-Bohm 效應

學生:陳光胤　　指導教授:褚德三

國立交通大學物理研究所

摘要

在本論文中，我們提出一個理論模型，來研究近來利用自組裝法(self-assembled)所製造出的同心量子雙環。我們利用電子在量子單環的確切解來形成一組基底，展開同心量子雙環之漢密頓函數(Hamiltonian)，並用數值方法將其對角化，得出相應的能量本徵值和本徵函數。藉由此法，我們可以研究 Aharonov-Bohm 效應，是否還會發生在中心有外加磁通量的量子雙環中？此外，我們也計算了在量子雙環中存在一個固定的雜質時之能階變化情形，並進一步討論量子環中有兩個對稱且固定的雜質，皆位於內環以及其一在內環而另一在外環的不同情形之能階變化。

Aharonov-Bohm Effect In Quantum Rings

Student: Guang-Yin Chen Adviser: Der-San Chuu

Institute of Physics
National Chiao Tung University

June, 2006

Abstract

In this thesis, we propose a theoretical model to study the spectra of the concentric quantum rings which have been fabricated lately by self-assembled technique. By using the exact diagonalization method, we examine whether the Aharonov-Bohm (AB) effect still appears in the concentric quantum rings threaded by a magnetic flux. Moreover, we study the variations of the energy spectra when impurities are presented in the rings.

Contents

Chapter 1

Introduction

During the past two decades, ringlike structures, with the capability of trapping magnetic flux in their interiors, are regarded as the idea candidates for observing Aharonov-Bohm effect [1], such as the energy oscillations and persistent currents. The first observation of AB effect in normal metal rings was reported by Webb *et al.* [2]. Cheung *et al.* [3] calculated the persistent currents and the energy levels of the electron in a one-dimensional ring with impurities, and it reveals that in the presence of impurities, the gaps-like structures take place in energy spectra. In 1995, A. V. Chaplik [4] considered an opening (antidot) in a two-dimensional (2D) electron gas in a strong perpendicular magnetic field and found that the possibility of electron-to-hole tunneling around the antidot results in a shift for each of the excitonic levels, which oscillate as functions of the magnetic field. It is the first prediction for AB oscillation of excitonic levels in one-dimensional quantum ring structures. Römer and Raikh [6] then found similar results with a short-ranged interaction potential by using a quite different analytical approach. Rapid progress in nanostructure technology, especially self-assembly techniques, can produce nanoscopic semiconductor rings with a characteristic inner/outer radius of 10/30-70 nm, and 2-3 nm in height [6,7], and the AB oscillations in the ground state energy have been observed by Lorke *et al.* [7]. Song and Ulloa [8] studied the magnetic field effect on excitons in a finite width nanoring instead of a perfect one-dimensional quantum ring, and found that the excitons in nanorings behave like a great extent as those in quantum dots of similar dimensions. The finite width of nanorings can suppress completely the AB effect predicted for one-dimensional rings, Hu *et al.* [9] found similar results by numerically diagonalizing the effective-mass Hamiltonian of the problem. Zhu *et al.* [10] investigated the energy spectra and AB effect in a two dimensional quantum nanoring interrupted by two identical barriers and found that AB oscillation of energy spectra are strongly affected by the

double barriers: the fewer barriers the ring contains, the stronger the AB oscillation is.

From these previous works, one knows that the problems of the single quantum ring have been studied extensively both theoretically and experimentally. In 2005, Mano *et al.* [11] demonstrated the self-assembled formation of concentric quantum rings with high uniformity and excellent rotational symmetry using the droplet epitaxy technique. The diameters of the inner and outer rings are 45 ($\pm$3)nm and 100 ($\pm$5)nm, respectively; both rings are 3 ($\pm$1)nm high, and show a good circular symmetry. This report inspires us to consider a theoretical model to study this concentric quantum double ring. Because of the special geometry of the inner and outer rings, we would like to deal with problems of identical double impurities located both in the inner ring, or one in the inner ring and the other in the outer ring individually. This should be the most difference between the single quantum ring and the concentric quantum rings.

Chapter 2

Formulation

2.1 Single Quantum Ring

The hard-wall confinement potential is assumed for numerical calculations (Fig.2.1). The potential energy of this system can be written as

$$V = \begin{cases} \infty, & \text{if } r_a < r < r_b \\ 0, & \text{otherwise.} \end{cases}; \tag{2.1}$$

where $r_a(r_b)$ denotes the inner (outer) radius of the ring structure. The Hamiltonian of this system can then be written as

$$\hat{H}_e = \frac{\hat{p}_e^2}{2m_e^*} + \hat{V}, \tag{2.2}$$

where the subscription "e" denotes electron, and " m_e^* " is the effective mass of electron in the material. The appropriate Schrödinger equation of the electron of this "ring" system in polar coordinate then reads

$$\hat{H}_e\psi(r,\phi) = E\psi(r,\phi). \tag{2.3}$$

Because of $V(\vec{r}) = V(r)$, the solution of the equation can be written as the form of $\psi(r,\phi) = R(r)\Phi(\phi)$. Performing the separation of variables in the Schrödinger equation, the radial part is

$$-\frac{\hbar}{2m_e^*}(\frac{d^2}{dr^2} + \frac{1}{r}\frac{dR(r)}{dr}) + \frac{\hbar^2 m^2}{2m_e^* r^2}R(r) = ER(r), \tag{2.4}$$

where m is the angular momentum quantum number. It can also be written in terms of the dimensionless variable $u = kr$ (where $k = \sqrt{\frac{2m_e^* E}{\hbar^2}}$):

$$\frac{d^2R(u)}{du^2} + \frac{1}{u}\frac{dR(u)}{du} + (1 - \frac{m^2}{u^2})R(u) = 0. \tag{2.5}$$

The above equation can be recognized from the mathematical literature as Bessel's equation. The solution of the radial part of the wave function is $R(r) = C_1 J_{|m|}(kr) + C_2 Y_{|m|}(kr)$, where$J_{|m|}$ and $Y_{|m|}$ are the regular and irregular solution of cylindrical *Bessel* functions of order m, and C_1, C_2 are undetermined constant.

The angular part of the Schrödinger equation is

$$\frac{d^2\Phi(\phi)}{d\phi^2} + m^2\Phi(\phi) = 0. \tag{2.6}$$

The wave function of the angular part is $\frac{1}{\sqrt{2\pi}} e^{im\phi}$ ($m = 0, \pm 1, \pm 2, \pm 3...$). Particles for $|m|$ and $-|m|$ have the same quantized energies. Therefore, every energy level is twofold degenerate for each m except for $m = 0$. Consequently, the basis set for the electron in such a ring is given by products of the radial and angular parts, namely

$$\psi_{n,m}(r, \phi) = [C_1 J_{|m|}(kr) + C_2 Y_{|m|}(kr)] \cdot (\frac{1}{\sqrt{2\pi}} e^{im\phi}), \tag{2.7}$$

along with the normalization condition for the corresponding probability density ,

$$\int_{r_a}^{r_b} r dr \int_0^{2\pi} d\phi |\psi(r, \phi)|^2 = 1. \tag{2.8}$$

This condition is associated with the fact that the probability of finding the electron simultaneously in the small coordinate intervals $(r, r + dr)$ and $(\phi, \phi + d\phi)$.The boundary conditions at the edge of the well are satisfied for all values of ϕ, provided that

$$\begin{cases} C_1 J_{|m|}(kr_a) + C_2 Y_{|m|}(kr_a) = 0 \\ C_1 J_{|m|}(kr_b) + C_2 Y_{|m|}(kr_b) = 0 \end{cases}, \tag{2.9}$$

namely,

$$-\frac{C_1}{C_2} = \frac{Y_{|m|}(kr_a)}{J_{|m|}(kr_a)} = \frac{Y_{|m|}(kr_b)}{J_{|m|}(kr_b)}. \tag{2.10}$$

From this, one can determine the nth($n = 1, 2, 3...$) energy level and the value of $-\frac{C_1}{C_2}$ for this system. One thus has two quantum numbers for this two dimensional "ring" system (n, m), and the energy eigenvalues read

$$E_{n,m} = \frac{\hbar^2 k^2_{(n,m)}}{2m_e^*}. \tag{2.11}$$

The ground state and the first excited state wave functions are shown in Fig. 2.2 .

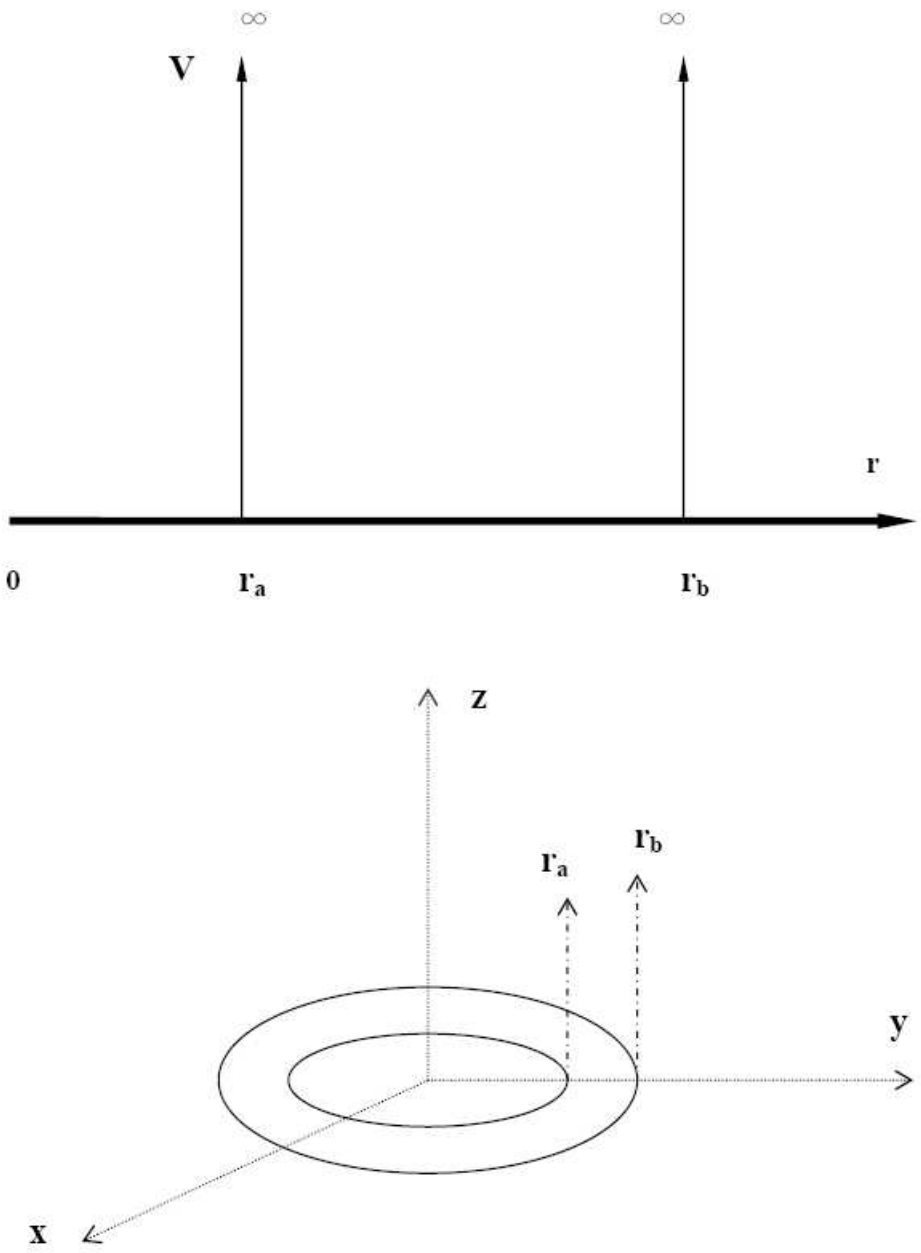

Figure 2.1: Radial view of potential (upper) and the quantum ring(bottom).

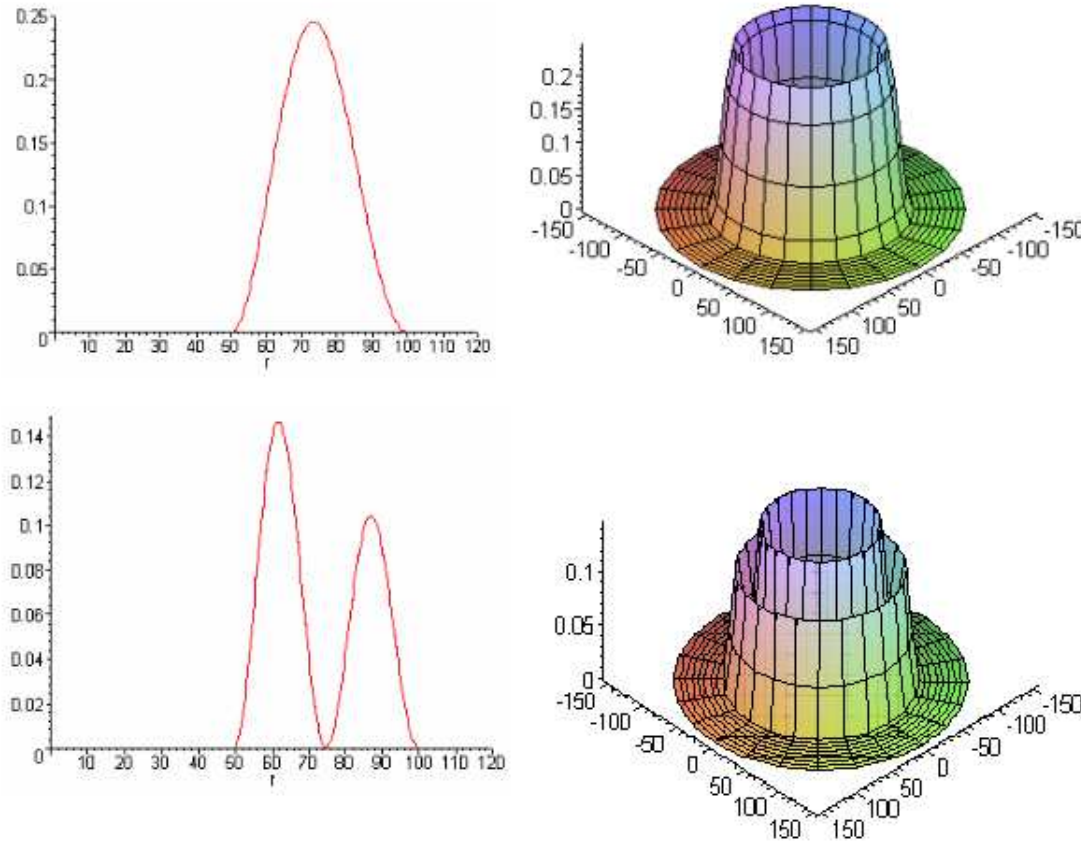

Figure 2.2: Upper panel: radial (left) and 3-dim (right) view of the ground state wave function of the quantum ring electron. Bottom panel: radial (left) and 3-dim(right) view of the first excited state wave function of a quantum ring electron (for $r_a = 50nm$ and $r_b = 100nm$).

2.2 Aharonov-Bohm Effect in Single Quantum Ring

Now let us consider a modified arrangement, where the ring shell encloses a uniform magnetic field, as shown in Fig.2.3. Intuitively we may conjecture that the energy spectrum is unchanged because the region with $\vec{B}(B\hat{z}) \neq 0$ is completely inaccessible to the charged particle trapped inside the ring. However, quantum mechanics tells us that this conjecture is not correct. Even though the magnetic field vanishes in the interior of the ring, the vector potential $\vec{A}$ is nonvanishing there. By using Stokes' theorem :

$$\oint_C \vec{A} \cdot d\vec{l} = \int\int_S (\vec{\bigtriangledown} \times \vec{A}) \cdot d\vec{S} = \int\int \vec{B} \cdot d\vec{S} = \Phi_B, \tag{2.12}$$

the vector potential $\vec{A} = (A_r, A_\phi, A_z)$ for the production of the magnetic field $\vec{B} = (B\hat{z})$ is

$$A_r = 0, A_\phi = \frac{\Phi_B}{2\pi r} = \frac{Br_a^2}{2r}, \ and \ A_z = 0 \ (\Phi_B \equiv B\pi r_a^2). \tag{2.13}$$

The Hamiltonian for a particle of electric charge q subjected to the magnetic field is

$$H = \frac{(\vec{P} + \frac{q\vec{A}}{c})^2}{2m_e^*} + V, \tag{2.14}$$

where $\vec{P}$ is canonical momentum which becomes an operator in quantum mechanics [12]. So, the Hamiltonian operator in the polar coordinate inside the ring ($\hat{V} = 0$) is

$$\begin{aligned} \hat{H} &= \frac{\hat{P}_r^{\,2}}{2m_e^*} + \frac{(\hat{P}_\phi - \frac{qA_\phi}{c})^2}{2m_e^*} \\ &= \frac{\hat{P}_r^{\,2}}{2m_e^*} + \frac{1}{2m_e^* r^2}(-i\hbar\frac{\partial}{\partial\phi} - \frac{qA_\phi r}{c})^2 \\ &= -\frac{\hbar}{2m_e^*}(\frac{d^2}{dr^2} + \frac{1}{r}\frac{d}{dr}) - \frac{\hbar^2}{2m_e^* r^2}(\frac{\partial}{\partial\phi} - \frac{q\Phi_B}{2\pi\hbar c})^2. \end{aligned} \tag{2.15}$$

If we consider that the ring width $(r_b - r_a)$ is zero, namely the ring is exactly an ideal one-dimensional ring, the energies will be independent of quantum number n, and the corresponding wavefunctions are

$$\psi_{n,m}(r,\phi) = [C_1 J_{|m|}(kr) + C_2 Y_{|m|}(kr)] \cdot (\frac{1}{\sqrt{2\pi}} e^{im\phi}).$$

We then have

$$\hat{H}\psi_{n,m} = E_m\psi_{n,m}$$

$$\Rightarrow -\frac{\hbar^2}{2m_e^* r^2}(\frac{\partial}{\partial\phi} - \frac{q\Phi_B}{2\pi\hbar c})^2\psi_{n,m} = E_m\psi$$

$$\Rightarrow E_m = \frac{\hbar^2}{2m_e^* r^2}(m - \frac{q\Phi_B}{2\pi\hbar c})^2. \tag{2.16}$$

For $q = -e$,

$$E_m = \frac{\hbar^2}{2m_e^* r^2}(m + \frac{\Phi_B}{\Phi_0})^2; m = 0, \pm1, \pm2, \pm3, .., \tag{2.17}$$

with Φ_0 being the universal flux quantum $\frac{hc}{e}$. Thus, with the increasing of the magnetic field, the ground state will change from angular momentum $m = 0$ to lower (negative) values of m (Fig.2.4) [2]. This phenomenon is the so-called "**Aharonov-Bohm-type oscillation**". It's a purely "quantum mechanical" phase interference effect, because the motion of a charged particle is determined solely by the Lorentz force. But in this problem, the charged particle bounded by the hard wall can never enter the region in which **B** is finite. The Lorentz force is identically zero in the regions where the particle wave function is finite. This point has led some people to conclude that in quantum mechanics, it is **A** rather than **B** that is more fundamental. Therefore, when a flux $\Phi_B = \pi r_a^2 B$ penetrates the interior of the ring, an additional phase contributed from **A** is picked up by the electron on its way around the ring and results in the "**Aharonov-Bohm effect** ".

Figure 2.3: A flux $\Phi_B = \pi r_a^2 B$ threads the interior of the ring.

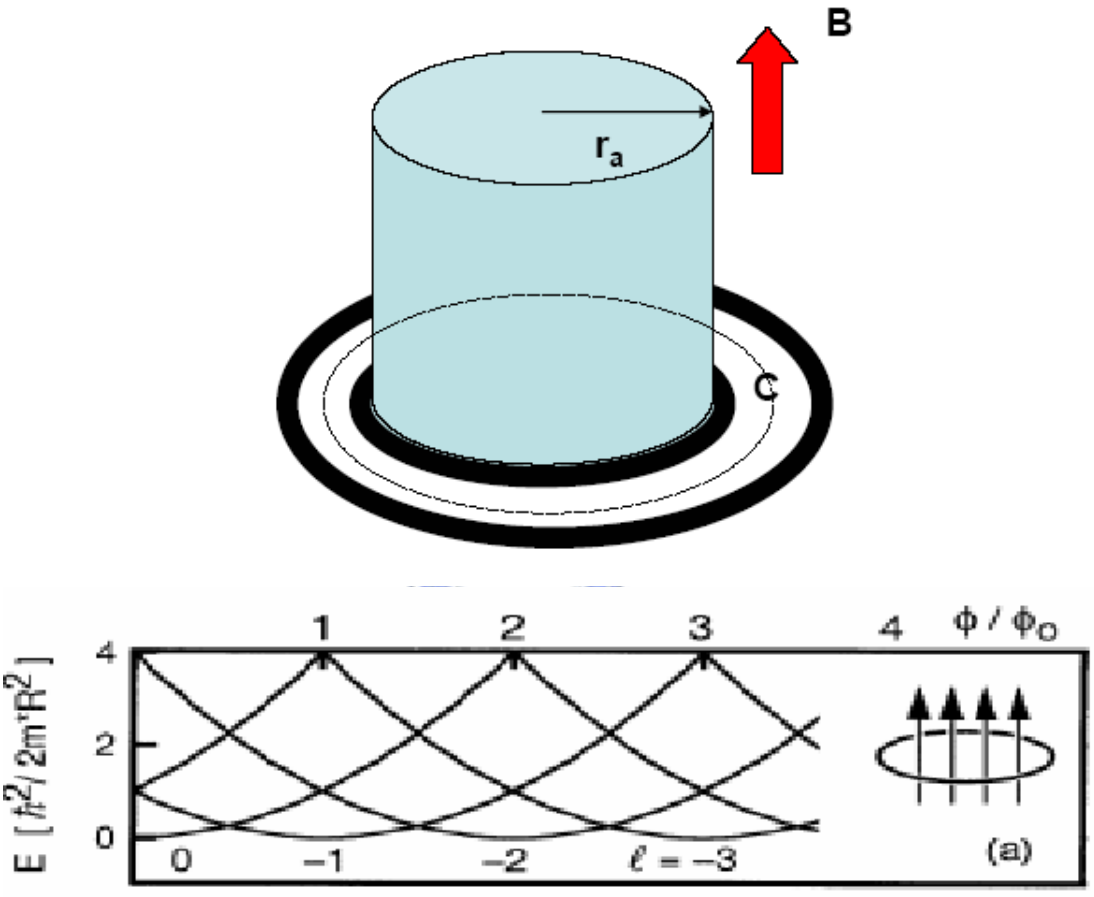

Figure 2.4: Energy levels of an ideal one dimensional ring as a function of the magnetic flux Φ_B threading the ring area. [A. Lork, R.J. Luyken, A.o. Govorov, J.P. Kotthaus, J.M. Garcia, and P.M. Petroff, Phys. Rev. Lett. **84**, 2223 (2000)].

2.3 Energy Spectra of Quantum Rings with Impurities

If we consider the energy spectra of a quantum ring with fixed impurities [3,10], in general, the interaction between an electron inside the ring and a fixed impurity is exactly the coulomb interaction (see Fig.2.5), and the corresponding potential energy U is

$$U = \frac{-e \cdot q_i}{\epsilon_r |\vec{r}_e - \vec{r}_i|},$$

where ϵ_r is the dielectric constant of media, and q_i is the charge of the impurity. Due to the coulomb interaction between a fixed impurity and an electron, the cylindrical symmetry (or the axial symmetry) will be broken, and the two-folded energy degeneracies for each m ($\pm|m|, |m| \neq 0$) will also be removed. Furthermore, because of the periodic boundary condition of the ring structure, this coulomb interaction is a periodic interaction to an electron circulating around a ring. As a result, the AB effect is reduced and the sawtooth-like oscillation is rounded with the presence of fixed impurities. There is a close connection between the states of an electron in a ring and the one-dimensional **Bloch** problem by comparing $2\pi\Phi_B/\Phi_0$ and kL [13] (k is the wave vector, and L is the length of the 1-dim. lattice). The energy levels of the ring form microbands as a function of Φ_B with period Φ_0, which is analogous to the Bloch electron bands in the extended k -zone picture.

Instead of the charged impurity, another type of the impurity is the barrier-like impurity (see Fig.2.5). For example, the formulation of the potential energy for two identical sectorial barriers is

$$V_g = \begin{cases} V_i, \theta \in [\pi - \frac{\alpha}{2} - \beta, \pi - \frac{\alpha}{2}] \\ \text{and} [\pi + \frac{\alpha}{2}, \pi + \frac{\alpha}{2} + \beta]; \\ 0, \text{otherwise.} \end{cases} .$$

These barriers can also break the cylindrical symmetry and remove the energy degeneracies. Fig.2.6 shows the energy spectra for a quantum ring with single barrier, two identical symmetric, or unsymmetrical barriers. From Fig.2.4 and Fig.2.6, one can find that in the absence of impurities (barriers), the curves form intersecting parabolas, however, in the presence of impurities, the **gaps** are opened at the points of intersection, just like the band structures in solid state physics.

It is clearly shown that the fewer impurities the ring contains, the stronger the AB oscillation is. In general, for rings containing two barriers, those with parallel double barriers have stronger AB oscillations than those with

nonparallel double barriers. In our latter discussions in this paper, we will also consider two concentric quantum rings with impurities. It will be more interesting than the single quantum ring, because in the case of concentric quantum rings, one can discuss the energy spectra of impurities located in different rings .

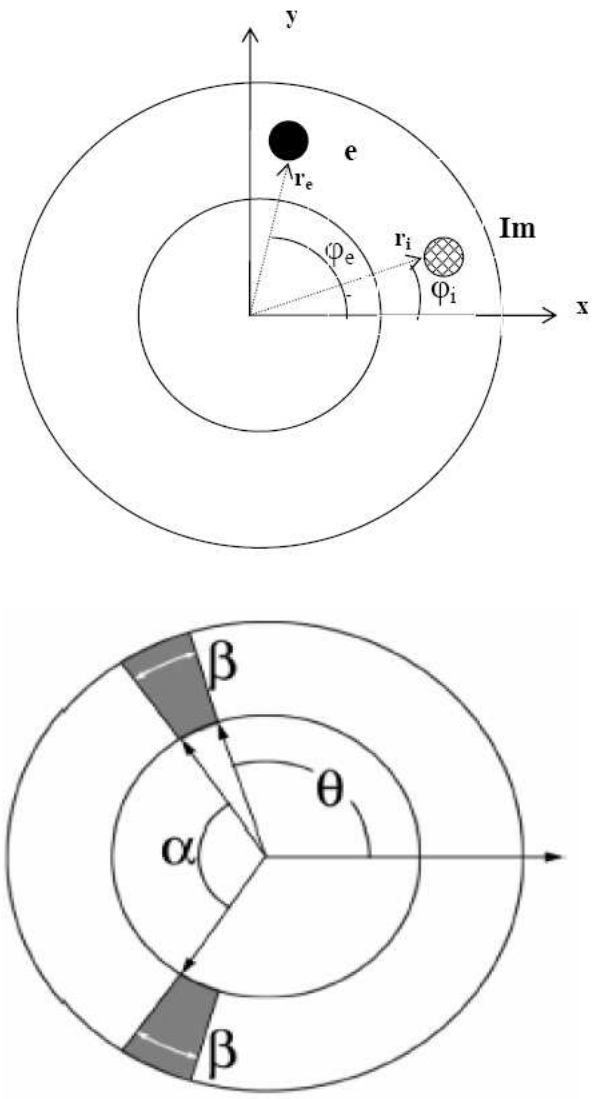

Figure 2.5: Upper panel: schematic view of a quantum ring with a fixed impurity. ϕ_e and ϕ_i denote the angle of electron and impurity, respectively. r_e denotes the radius of the electron. Bottom panel: schematic view of a quantum ring with double barrier.

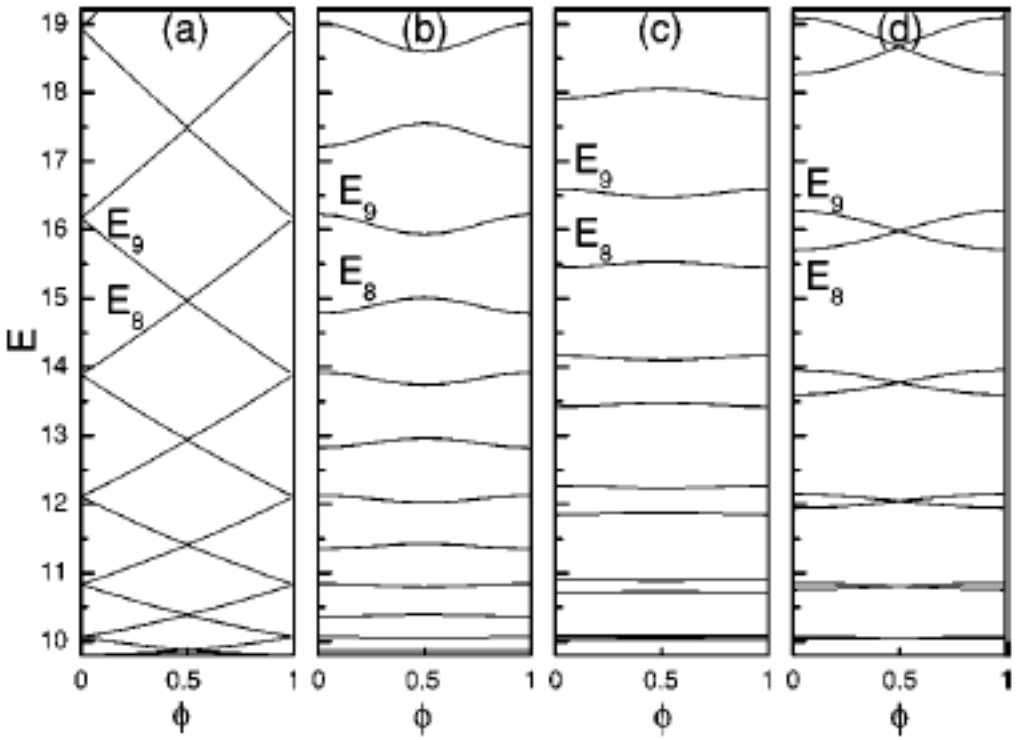

Figure 2.6: Energy spectra of a quantum ring as a function of the magnetic flux Φ_B: (a) without barrier(or impurity) structures, (b) with a single barrier, (c) nonparallel double barriers, and (d) parallel double barriers (Zhu et al., Phys. Rev. B **67**, 075404 (2003)).

2.4 Theoretical Model for Two Concentric Quantum Rings

In section 2.1 and 2.2, we have introduced the basic concepts of quantum rings and discussed how AB effect takes place when a finite magnetic flux exist, in the region bounded by the ring. In 2004, Mano *et al.* [11] demonstrated two self-assembled concentric quantum rings with high uniformity and excellent rotational symmetry using the droplet epitaxy technique. It inspires us to consider whether the AB effect still takes place in the concentric quantum rings. We thus consider a simple model to fit the potential energy(see Fig.2.7) of two concentric quantum rings. The hard-wall confinement potential is used to simulate the "single" quantum ring in sec.2.1. In order to simulate the concentric quantum rings here, one finite potential barrier V_0 is included in the middle of radial direction (from r_c to r_d). Thus, the potential energy V_c of the concentric quantum double rings becomes :

$$V' = V(eq.2.1) + V_b = \begin{cases} \infty, & \text{if } r_a < r < r_b; \\ V_0, & \text{if } r_c < r < r_d; \\ 0, & \text{otherwise.} \end{cases}, \tag{2.18}$$

where the added barrier V_b is

$$V_b = \begin{cases} V_0, & \text{if } r_c < r < r_d; \\ 0, & \text{otherwise.} \end{cases}. \tag{2.19}$$

Since

$$\int_{r_a}^{r_b} r dr \int_0^{2\pi} d\phi \psi^*_{n',m'} \psi_{n,m} = \delta_{n,n'} \delta_{m,m'}, \tag{2.20}$$

the eigenkets $|n, m\rangle$ (the $\psi_{n,m}$ in sec.2.1) of single quantum ring form a complete(orthonormal) set with the completeness relation

$$\sum_{n,m} |n, m\rangle\langle n, m| = \hat{1}. \tag{2.21}$$

Because the boundary of the single quantum ring and the concentric quantum rings are the same, so we can take the complete set of the single quantum ring to be the basis to span the eigenspace of any physical operators of the concentric quantum double ring. Therefore, a physical operator $\hat{O}$ is represented as

$$\hat{O} = \hat{1}\hat{O}\hat{1} = \sum_{n,m;n',m'} |n', m'\rangle\langle n', m'|\hat{O}|n, m\rangle\langle n, m| \tag{2.22}$$

$$\Rightarrow \hat{O} \doteq \begin{pmatrix} \langle n'=1,m'=0|\hat{O}|n=1,m=0\rangle & \langle n'=1,m'=0|\hat{O}|n=1,m=-1\rangle & \cdots \\ \langle n'=1,m'=-1|\hat{O}|n=1,m=0\rangle & \langle n'=1,m'=-1|\hat{O}|n=1,m=-1\rangle & \cdots \\ \vdots & \vdots & \ddots \\ \cdots & \cdots & \cdots \end{pmatrix}.$$

Since the boundary of quantum rings is hard-wall, the value of the principle quantum number n has no upper limit (n=1$\rightarrow \infty$), and because the magnetic quantum number m is independent of n, m also has no upper limit ($|m| = 0 \rightarrow \infty$). In our numerical calculations, we diagonalize the matrix of physical operators numerically. So, the number of basis should be truncated to make numerical calculations possible. Through checking the property of convergence of energy eigenvalues, we find that with up to 1010 elements ($n = 1 \rightarrow 10$ and $m = -50 \rightarrow 50$) of the basis, the energy eigenvalues converge to a constant even we keep adding element number. We will apply this numerical method to calculate the wave functions of a concentric quantum double ring with the use of the "effective Hatree unit" of atomic physics for GaAs materials. We also set

$$\begin{cases} r_a = 80nm(8a_B^*); \\ r_b = 100nm(10a_B^*); \\ r_c = 86nm(8.6a_B^*); \\ r_d = 94nm(9.4a_B^*). \end{cases}, \tag{2.23}$$

where $a_B^* = 4\pi\varepsilon_0\varepsilon_r\hbar^2/m_e^*e^2$ is the effective Bohr radius. Here, $a_B^* = 10nm$ and $\varepsilon_r = 10.9$ for the material of GaAs.

The Hamiltonian operator of a concentric quantum double ring is

$$\hat{H} = \frac{\hat{p}_e^2}{2m_e^*} + \hat{V}'. \tag{2.24}$$

According to Eq. (2.23), $\hat{H}$ can be written as

$$\hat{H} = \hat{1}\hat{H}\hat{1} = \sum_{n,m;n',m'} |n',m'\rangle\langle n',m'|\hat{H}|n,m\rangle\langle n,m| \tag{2.25}$$

$$\hat{H} \doteq \sum_{n,m;n',m'} \langle n',m'|\hat{H}|n,m\rangle. \tag{2.26}$$

Since we have represented the Hamiltonian operator by a 1010×1010 Hermitian square matrix, all we need to do is to diagonalize this matrix. We then get 1010 energy eigenvalues E_i ($i = 1 \rightarrow 1010$), and the corresponding eigenkets $|\Phi_i\rangle$ ($i = 1 \rightarrow 1010$). From linear algebra, every $|\Phi_i\rangle$ is a linear combination of $|n,m\rangle$, namely

$$|\Phi_i\rangle = \sum_{n,m} C_{n,m}|n,m\rangle, \tag{2.27}$$

where $C_{n,m}$ is the "weight" of corresponding $|n, m\rangle$, and we will get $C_{n,m}$ after diagonalizing the matrix of Hamiltonian (Eq. (2.26)).

The radial part's potential of the concentric quantum double rings is similar to 1-dim. symmetric double-well potential. However, since the radial part of a ring structure has no parity symmetry, the radial part's ground state wave function of the concentric quantum double ring is not symmetrical with respect to the middle barrier. Therefore, the probability density of the electron in the inner ring is higher than that in the outer ring (see Fig.2.10). From quantum mechanics, if the middle barrier V_0 is very high, there is rare possibility for the tunneling between the inner and outer ring (see Fig.2.8). So we set $V_0 = 100meV$ to make tunneling become possible (see Fig.2.8). Fig.2.9 illustrates the scheme of concentric quantum double ring and Fig.2.10 shows the ground state wave function $|\Phi_1\rangle$ of a concentric quantum double ring with the middle barrier $V_0 = 100meV$.

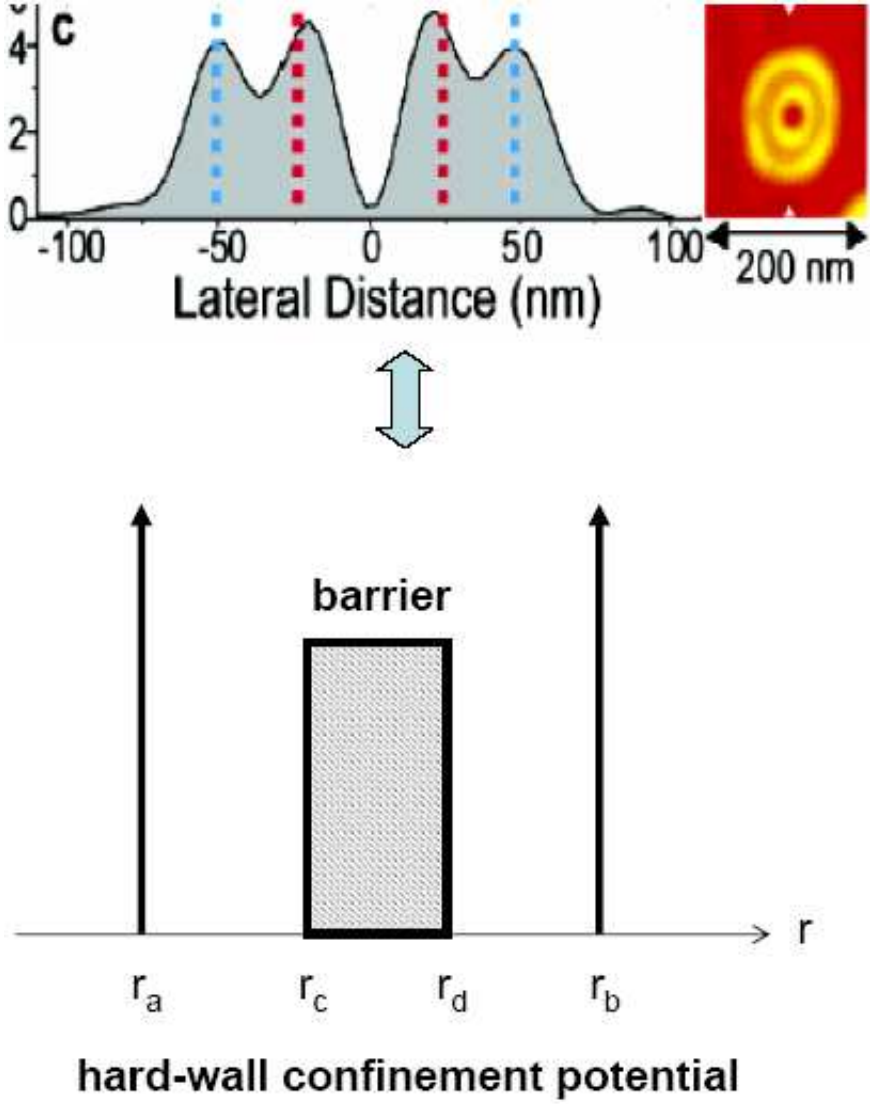

Figure 2.7: Illustration of the concentric quantum double ring in real space (upper panel) (Takaaki Mano et al., Nano Lett. **5**, 425 (2005)). Lower panel: theoretical model for the double-ring.

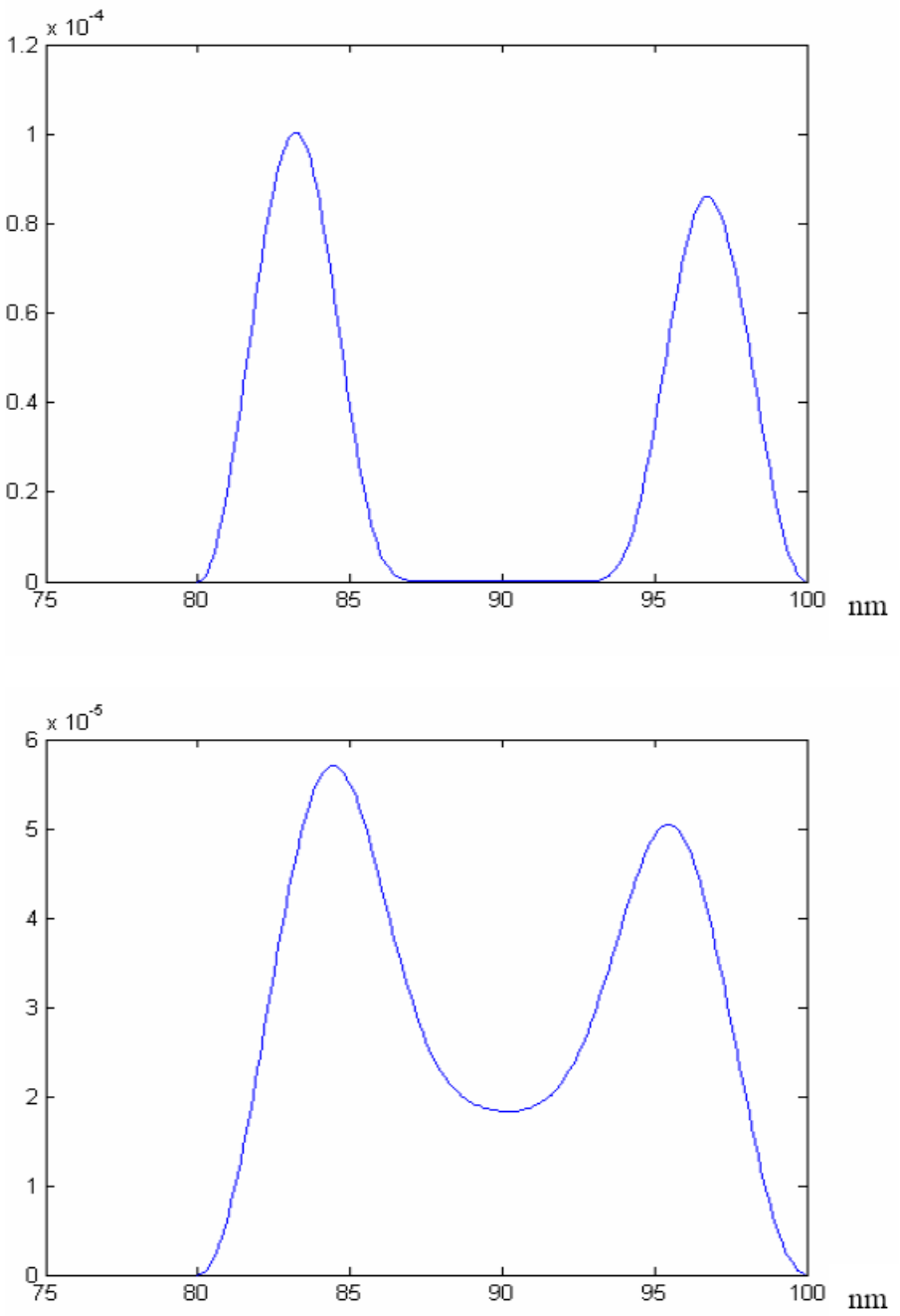

Figure 2.8: The ground state wave function (radial part) of a concentric quantum double ring for the middle barrier with height 300meV (upper) and 100meV(bottom).

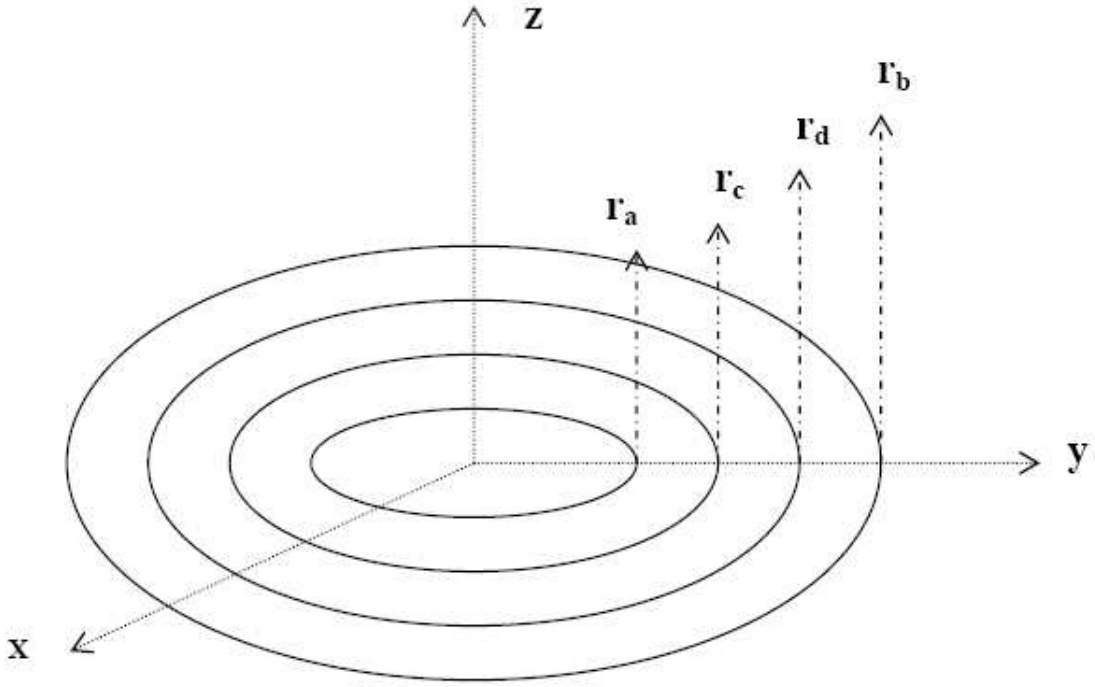

Figure 2.9: Illustration of the concentric quantum double ring

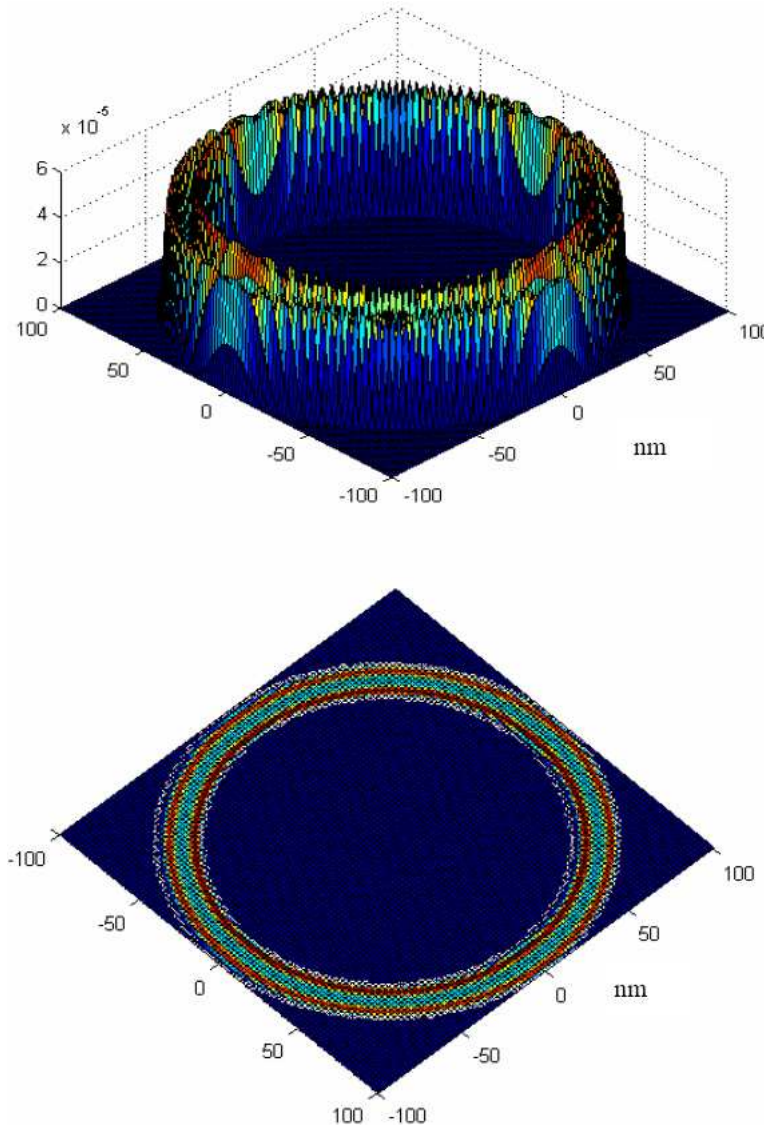

Figure 2.10: Upper panel : the ground state wave function of a concentric quantum double ring. Bottom panel : a vertical view of upper panel. The small red ring is the inner ring and the large red ring is the outer ring. The light green part is the middle barrier of the double ring.

Chapter 3

Results and Discussions

We have built a theoretical model to calculate the ground state wave function of the electron in concentric quantum double rings. In this chapter, we present the results and discussions on some physical properties such as AB effect, impurity binding energies, and the energy spectra of a concentric quantum double ring in the presence of impurities.

3.1 Aharonov-Bohm Effect in Concentric Quantum Rings

The Hamiltonian operator for a concentric quantum double ring is

$$\hat{H} = \frac{\hat{p}_e^2}{2m_e^*} + \hat{V}',$$

where $\hat{V}'$ is the same as Eq. (2.18). Let us consider the concentric quantum double ring acting by an interior-threaded uniform magnetic field oriented along the **z** axis. The corresponding vector potential is the same as Eq. (2.13), and the Hamiltonian is

$$H = \frac{(\vec{P} - \frac{q\vec{A}}{c})^2}{2m_e^*} + V'. \tag{3.1}$$

Inside the concentric quantum double ring , the Hamiltonian operator is :

$$\hat{H} = \frac{\hat{P_r}^2}{2m_e^*} + \frac{(\hat{P_\phi} - \frac{qA_\phi}{c})^2}{2m_e^*} + \hat{V_b}$$

$$= \frac{\hat{P_r}^2}{2m_e^*} + \frac{1}{2m_e^* r^2}(-i\hbar\frac{\partial}{\partial\phi} - \frac{qA_\phi r}{c})^2 + \hat{V_b}$$

$$= -\frac{\hbar}{2m_e^*}(\frac{d^2}{dr^2} + \frac{1}{r}\frac{d}{dr}) - \frac{\hbar^2}{2m_e^* r^2}(\frac{\partial}{\partial\phi} - \frac{q\Phi_B}{2\pi\hbar c})^2 + V_0 \ (if\, r_c < r < r_d), \quad (3.2)$$

where Eq. (3.2) is the Hamiltonian operator in position representation. We use this as the basis (1010 elements) to span the eigenspace of $\hat{H}$ and diagonalize the matrix of this Hamiltonian and obtain the corresponding 1010 energy eigenvalues $E_{n,m}$ ($E_{n,m} = E_n + E_m$), where $E_n = \frac{p_{r,n}^2}{2m_e^*}$, p_r is the momentum of the radial part, and n is the principle quantum number. As in Eq.(2.17), $E_m = \frac{\hbar^2}{2m_e^* r^2}(m + \frac{\Phi_B}{\Phi_0})^2$ with $\Phi_0 = \frac{hc}{e}$ and $\Phi_B = B\pi r_a^2$. More explicitly, $E_{n,m}$ is written as

$$E_{n,m} = \frac{p_{r,n}^2}{2m_e^*} + \frac{\hbar^2}{2m_e^* r^2}(m + \frac{\Phi_B}{\Phi_0})^2 \ (n = 1 \to 10; m = 0, \pm 1, \pm 2, .. \pm 50). \quad (3.3)$$

With the increasing of the magnetic field, the lowest energy of each n (i.e. $E_{n,m} = E_{1,0}, E_{2,0}, .., E_{n,0}$) should change from angular momentum $m = 0$ to lower m (negative value). It means AB effect should also take place in concentric quantum double rings, and our results (Fig.3.2), have confirmed this.

Note that all energies here are measured in units of the effective Rydberg $Ry^* = m_e^* e^4/2\hbar^2(4\pi\epsilon_0\epsilon_r)^2$, and all distances are measured in units of effective Bohr radius $a_B^* = 4\pi\varepsilon_0\varepsilon_r\hbar^2/m_e^* e^2$. For GaAs materials, $Ry^* = 5.8meV$, the effective mass of the electron is $0.067m_e$, and the universal flux quanta Φ_0 for a 1D ring with a radius a_B^* corresponds to the magnetic field of $13.18T$.

One might wonder that whether the tunneling of the electron between the inner and the outer ring affects the AB effect. To answer this, we raise the "height" of the middle barrier to 300meV to suppress the tunneling of the electron between the inner and the outer ring. It is found that the behavior of AB oscillation of energy spectra is the same as in Fig.3.2. We then conclude the tunneling effect does not affect the AB effect.

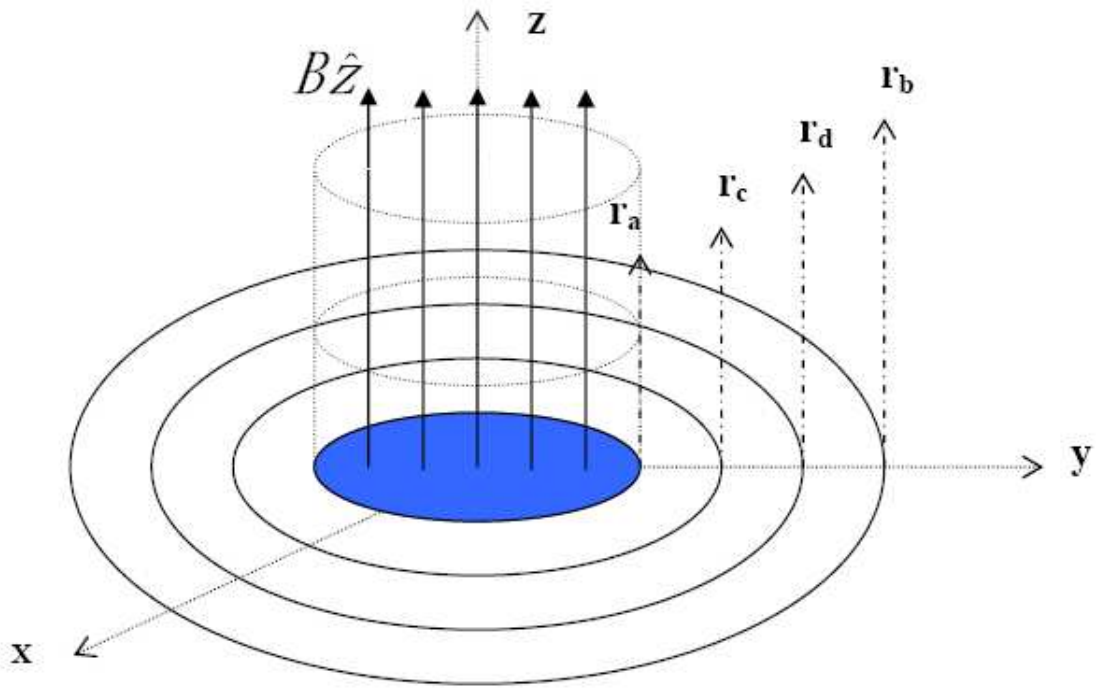

Figure 3.1: Illustration of the concentric quantum double ring with a interior-threaded constant magnetic field.

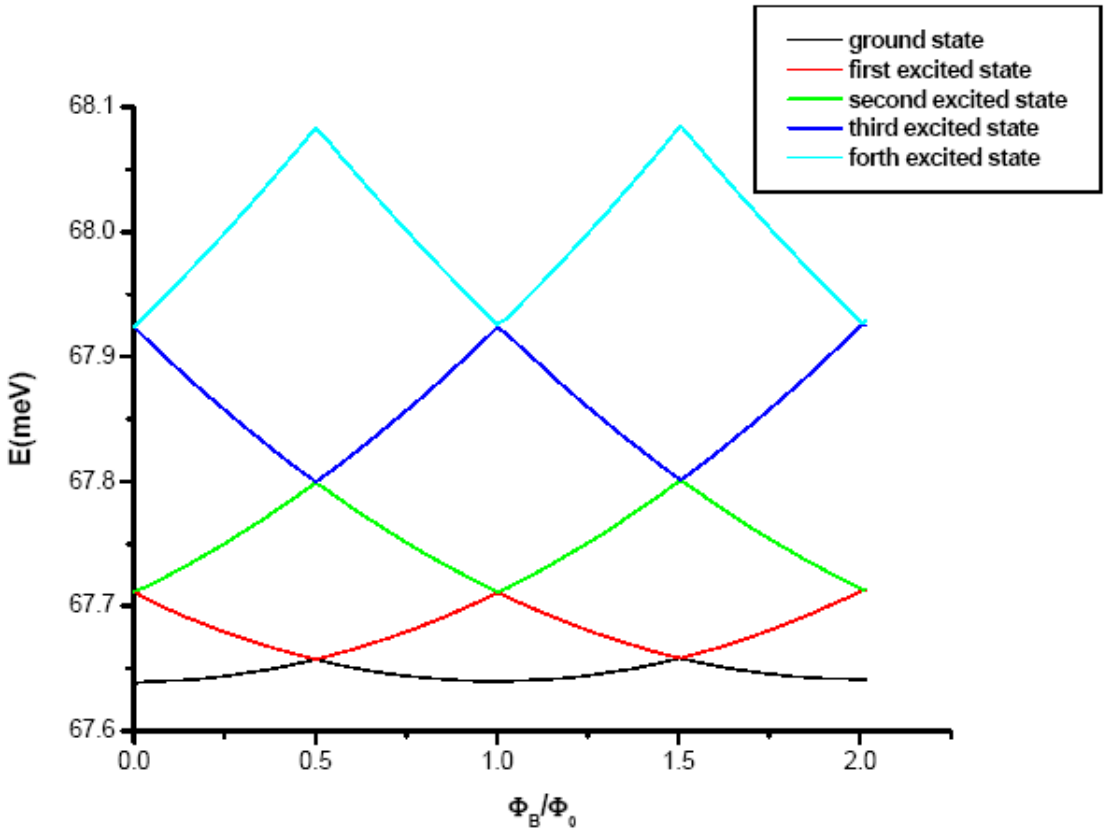

Figure 3.2: Energy levels of a concentric quantum double ring as a function of the magnetic flux Φ_B threading through the ring area.

3.2 Energy Spectra of Concentric Quantum Rings with Single Impurity

In this section, we are more concerned with the energy spectra of a concentric quantum double ring with one impurity inside the inner or outer ring. Let us consider one fixed impurity (charges $+|e|$) located in the middle of inner ring ($r_i = 83nm$). The azimuthal angle of this impurity is at $\phi_i = 0$, i.e. this impurity is on the **x** axis (see Fig.3.3). It is obvious that the electron rounding in a concentric quantum double ring would be strongly attracted by the fixed impurity as a result of the coulomb interaction between the impurity and electron without taking the electrical screening effect into account. So the probability density amplitude of the electron would gather around the position of the fixed impurity for low-lying energy states. In other words, the electron would be bounded by the impurity when the electron is in low-lying energy states (see Fig.3.4).

The Hamiltonian of a concentric quantum double ring with an impurity can be written as

$$\hat{H} = \frac{\hat{p}_e^2}{2m_e^*} - \frac{e^2}{\epsilon_r|\vec{r}_e - \vec{r}_i|} + \hat{V}', \tag{3.4}$$

where $|\vec{r}_e - \vec{r}_i|$ is the distance between the electron and the impurity. Applying the z-axis oriented uniform magnetic field threading the interior of the concentric quantum double ring as previous discussions, the Hamiltonian turns out to be

$$H = \frac{(\vec{P} - \frac{e\vec{A}}{c})}{2m_e^*} - \frac{e^2}{\epsilon_r|\vec{r}_e - \vec{r}_i|} + V'. \tag{3.5}$$

From Eq. (2.26), one can get the matrix representation of this Hamiltonian and diagonalize it numerically again. The total energy E_{tot} of this system is obtained as [14]

$$E_{tot} = E_{n,m} - E_b, \tag{3.6}$$

where the binding energy E_b is defined as

$$E_b \equiv E_{n,m} - E_{total} \text{ , and } E_b \geq 0. \tag{3.7}$$

As discussed in the last section, because of the AB effect, $E_{n,m}$ will oscillate periodically. But we find the total energy E_{tot} continually increases as one increases the magnitude of the uniform magnetic field. It seems that the AB effect doesn't happen in total energy. From Eq. (3.6), one may easily conject that E_b should oscillate periodically, but has non-fixed amplitude as shown in Fig. 3.5 and Fig. 3.6.

We now consider a more general situation. As is well known, the coulomb interaction will be reduced by the electrical screening from other atoms in materials. The field strength seen by the electron should not be so strong. Nevertheless, the impurity still breaks the cylindrical symmetry and lifts the two-folded energy degeneracies for each m ($\pm|m|, |m| \neq 0$) of the concentric quantum double rings. Instead of trapping the electron, the coulomb interaction due to the fixed impurity plays a role of providing a periodic potential, just like the Kronig-Penney model in the band structure problem. For simplicity, we reduce two orders of the strength of the coulomb interaction and apply the uniform magnetic field threading the interior of the ring to this system. We find that because of the periodic boundary condition due to the impurity, the band gaps appear at the points of intersection are as shown in Fig. 3.7.

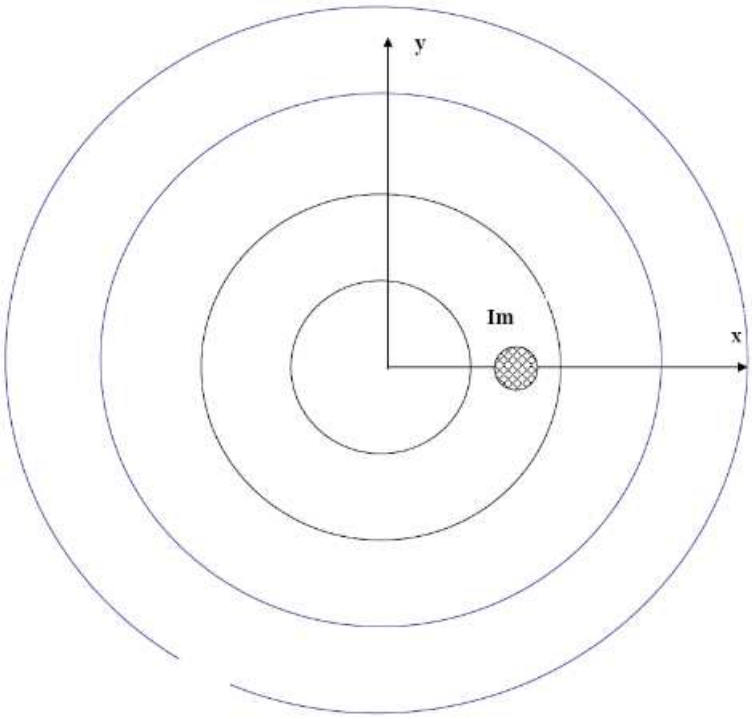

Figure 3.3: Illustration of a concentric quantum double ring with an impurity located at $r_i = 83nm$ and $\phi_i = 0$.

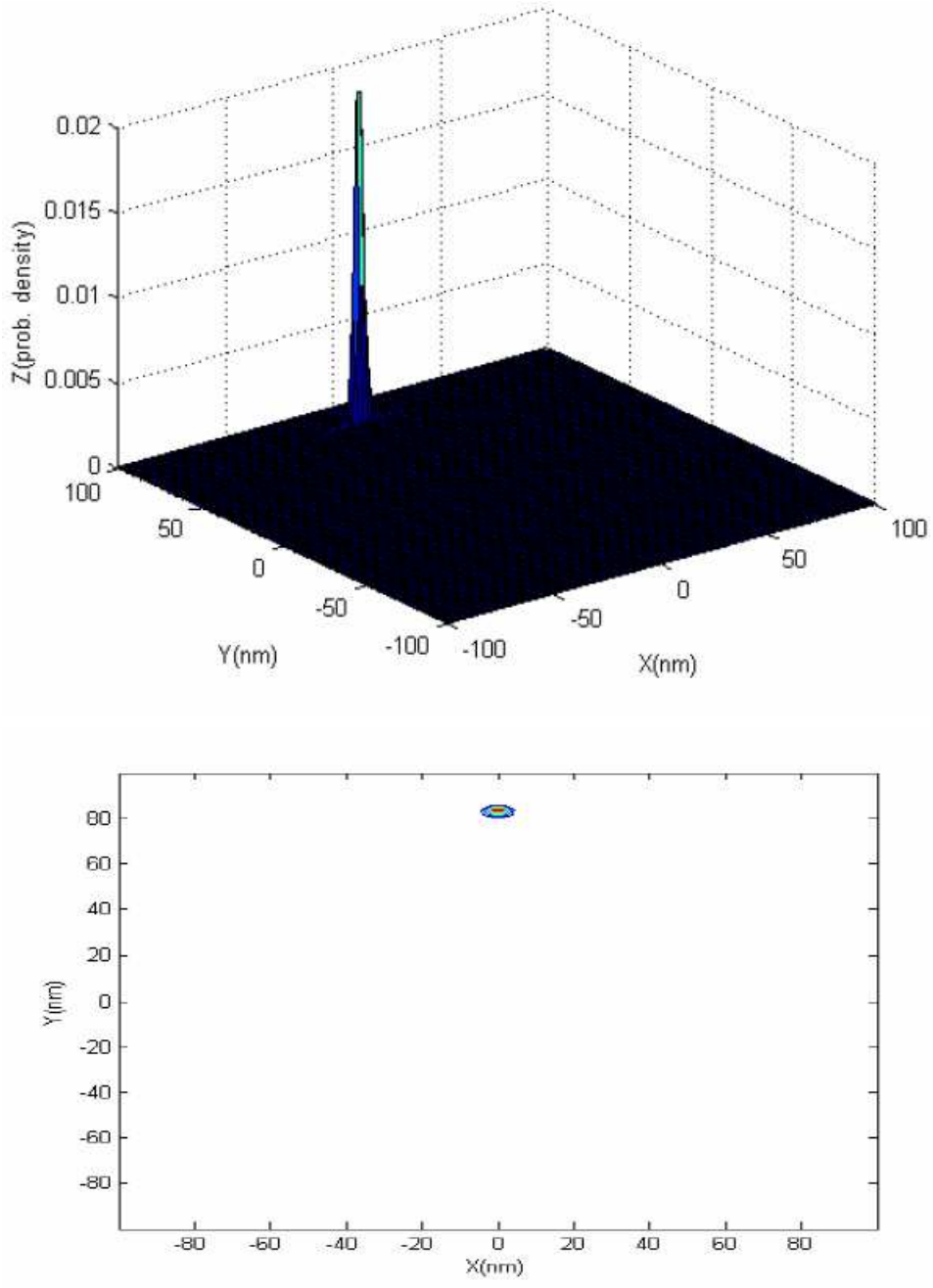

Figure 3.4: Upper panel : the ground state wave function of a concentric quantum double ring with an impurity. Bottom panel : a contour view of upper panel.

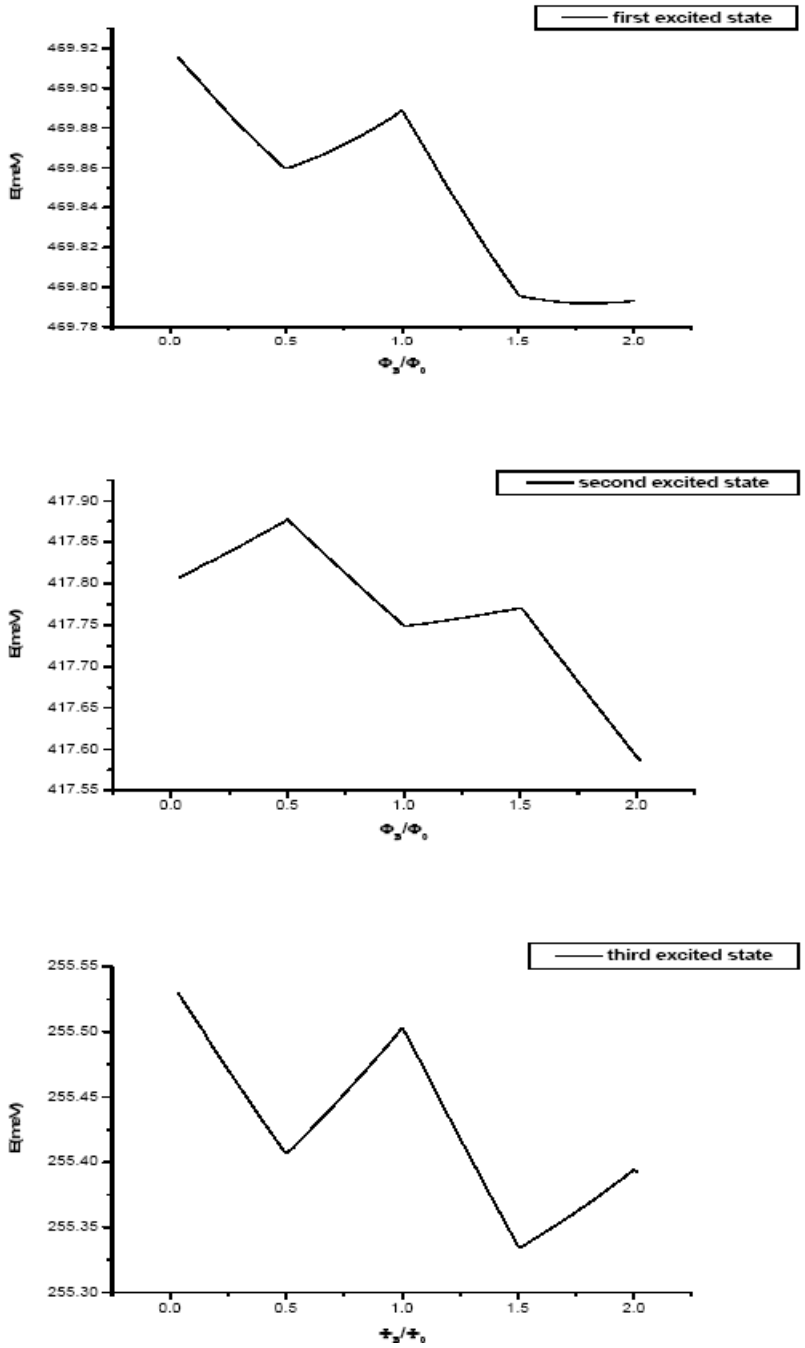

Figure 3.5: Oscillations of the binding energies of the first excited state (upper), the second excited state (middle), and the third excited state (bottom).

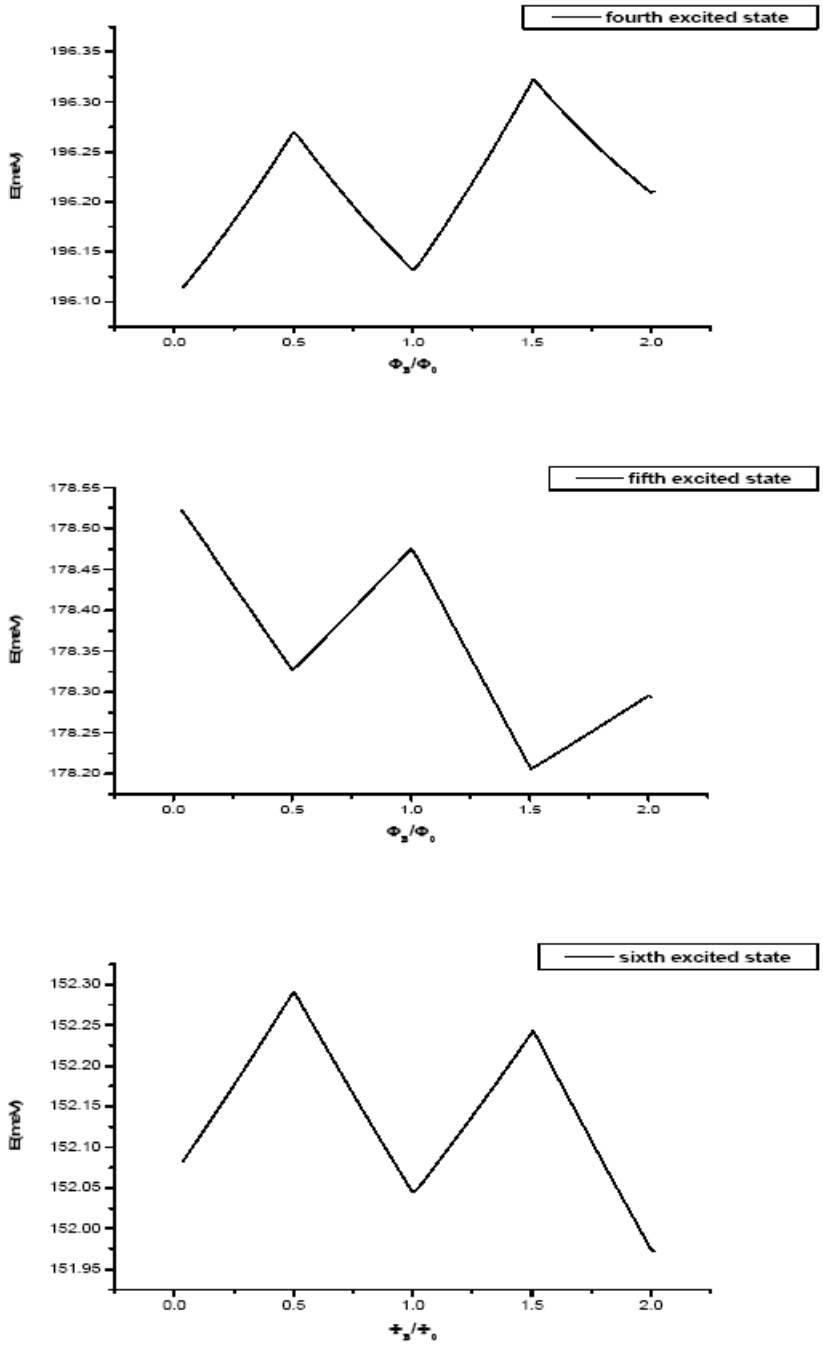

Figure 3.6: Oscillations of binding energies of the fourth excited state (upper), the fifth excited state (middle), and the sixth excited state (bottom).

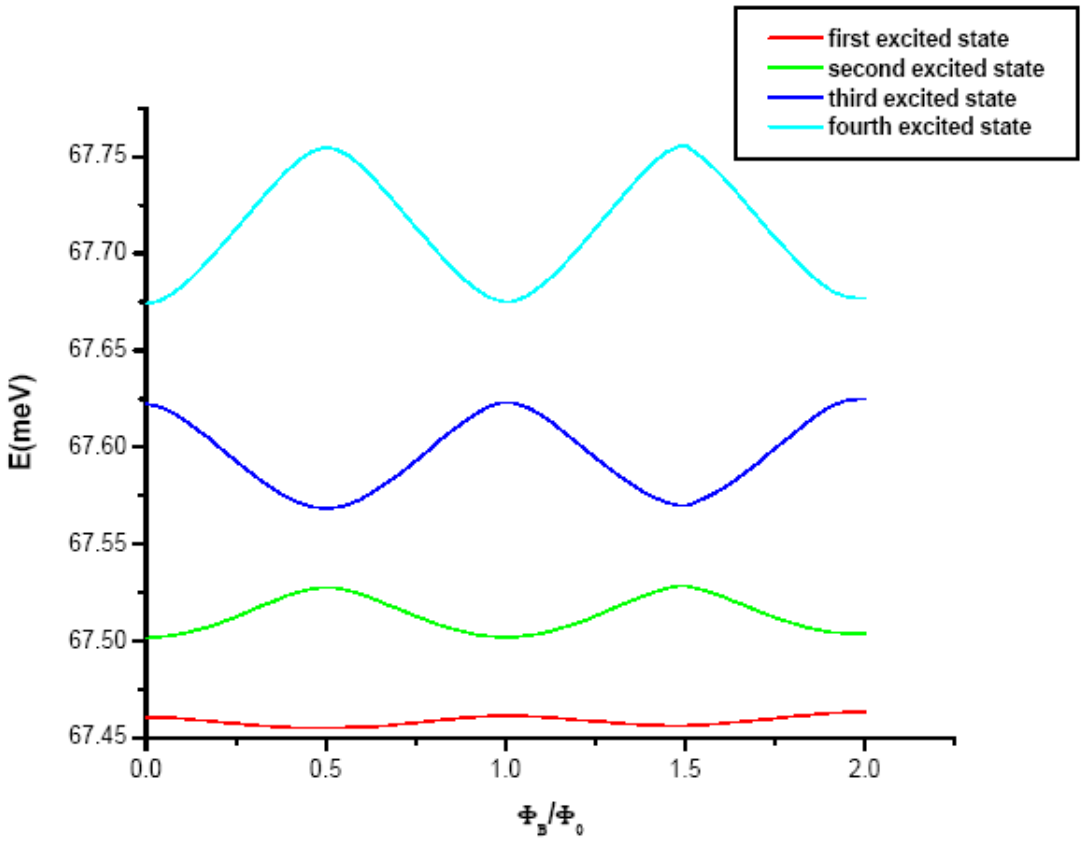

Figure 3.7: Energy spectra of a concentric quantum double ring with one impurity as a function of the magnetic flux Φ_B threading through the ring area.

3.3 Energy Spectra of Concentric Quantum Rings with Two Impurities

In last section, we deal with a concentric quantum double ring with single impurity. In this section, we would like to discuss the concentric quantum rings with two impurities. Since a concentric quantum double ring has two rings: inner and outer rings, one can put two identical impurities in two different rings individually, and see how the energy spectra varies.

Following the last section, we put another identical impurity also in the middle of inner ring with $\phi = \pi$. So the inner ring has two identical symmetric impurities at $\phi_{i1} = 0$ and $\phi_{i2} = \pi$ (Fig.3.8). The Hamiltonian now becomes

$$\hat{H} = \frac{\hat{p}_e^2}{2m_e^*} - \frac{e^2}{\epsilon_r|\vec{r}_e - \vec{r}_{i1}|} - \frac{e^2}{\epsilon_r|\vec{r}_e - \vec{r}_{i2}|} + \hat{V}'. \tag{3.8}$$

We also apply an uniform magnetic field threading the interior of the ring and find that the appearance of the second impurity located at $r_{i2} = 83nm$ and $\phi_{i2} = \pi$ results in the disappearance of energy gaps as shown in Fig.3.9. To explain this, one has to take a closer look at the second excited state $E_{1,1}$(the green curve), the third excited state $E_{1,-2}$ (the deep blue curve), and the the fourth excited state $E_{1,2}$ (the light blue curve). One finds that in the presence of the second impurity, the cylindrical symmetry is broken further. So the separation of $E_{1,-2}$ and $E_{1,2}$ is bigger than that with only one impurity inside the inner ring, and the separation of $E_{1,1}$ and the $E_{1,-2}$ becomes closer. Therefore, the energy gap between $E_{1,1}$ and $E_{1,-2}$ vanishes, and the curves of $E_{1,1}$ and $E_{1,-2}$ intersects again.

Because a concentric quantum double ring has one inner and outer rings, one can also consider the second impurity is put in the middle in the middle of the outer ring located at $r_{i2} = 97nm$ and $\phi_{i2} = \pi$ (Fig.3.10). In this case, these two impurities are not symmetric anymore in the radial direction, but still symmetric in the azimuthal angle part. From Fig.2.8, we realize that the radial wave function of a concentric quantum double ring is not symmetric with respect to the middle barrier, and an electron prefers to appear in the inner ring rather than in the outer ring. Thus, we are then able to conjecture that when the uniform magnetic field is applied, the energy levels $E_{1,1}$ and $E_{1,-2}$ should not intersect with each other because of the difference in the radial probability density for inner and outer rings. Fig.3.11 shows the energy spectra of $E_{1,1}$ and $E_{1,-2}$. Comparing it with Fig.3.9, the gaps appear, which proves our conjecture.

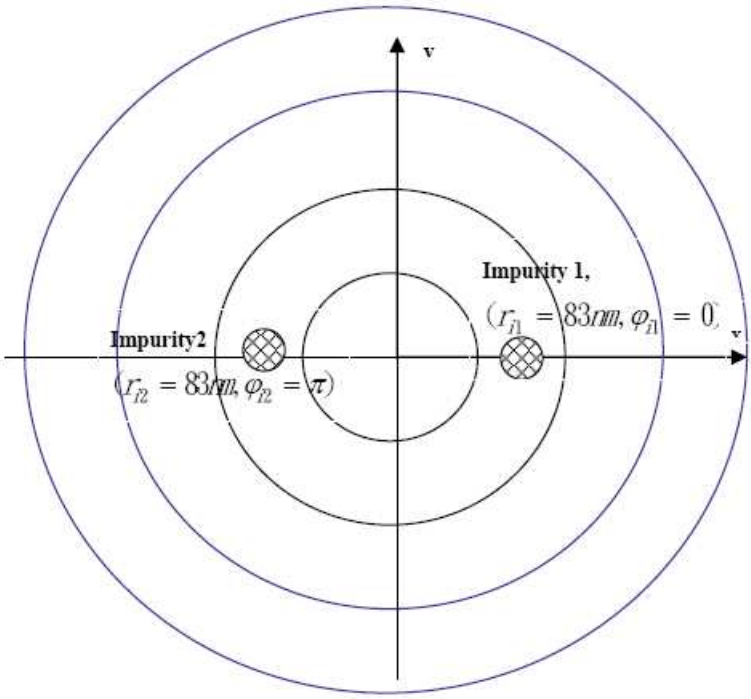

Figure 3.8: Illustration of a concentric quantum double ring with two identical symmetric impurities located at $(r_{i1} = 83nm, \phi_{i1} = 0)$ and $(r_{i2} = 83nm, \phi_{i2} = \pi)$.

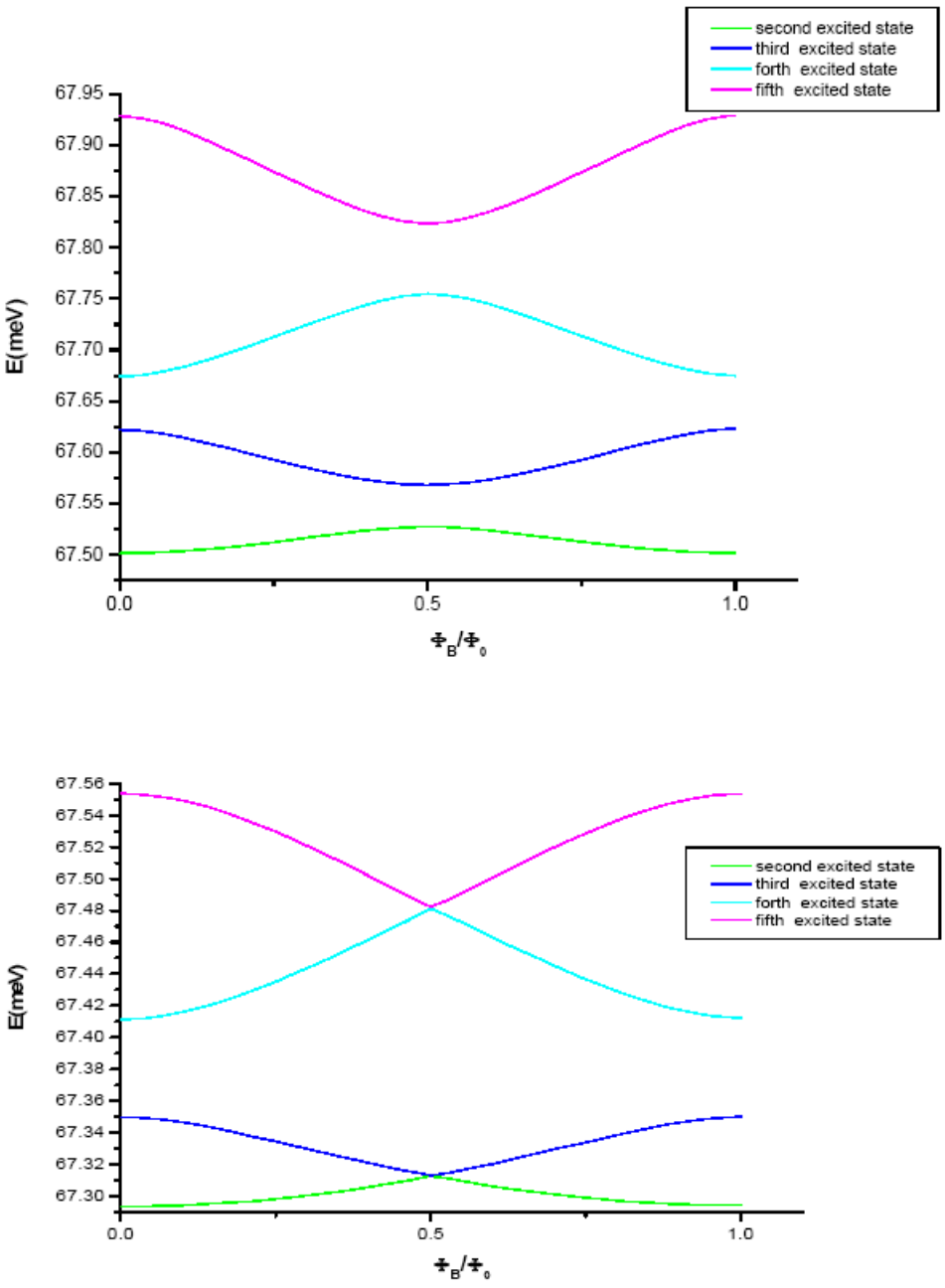

Figure 3.9: Upper panel : energy spectra of a concentric quantum double ring with single impurity. Bottom panel : energy spectra of a concentric quantum double ring with symmetric double impurities .

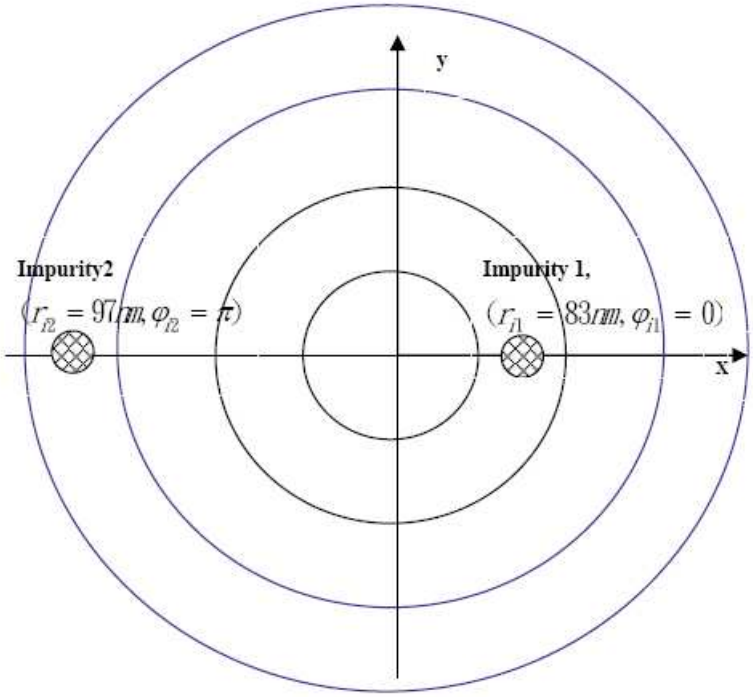

Figure 3.10: Illustration of a concentric quantum double ring with two identical symmetric impurities located at the inner ring ($r_{i1} = 83nm, \phi_{i1} = 0$) and the outer ring ($r_{i2} = 97nm, \phi_{i2} = \pi$) .

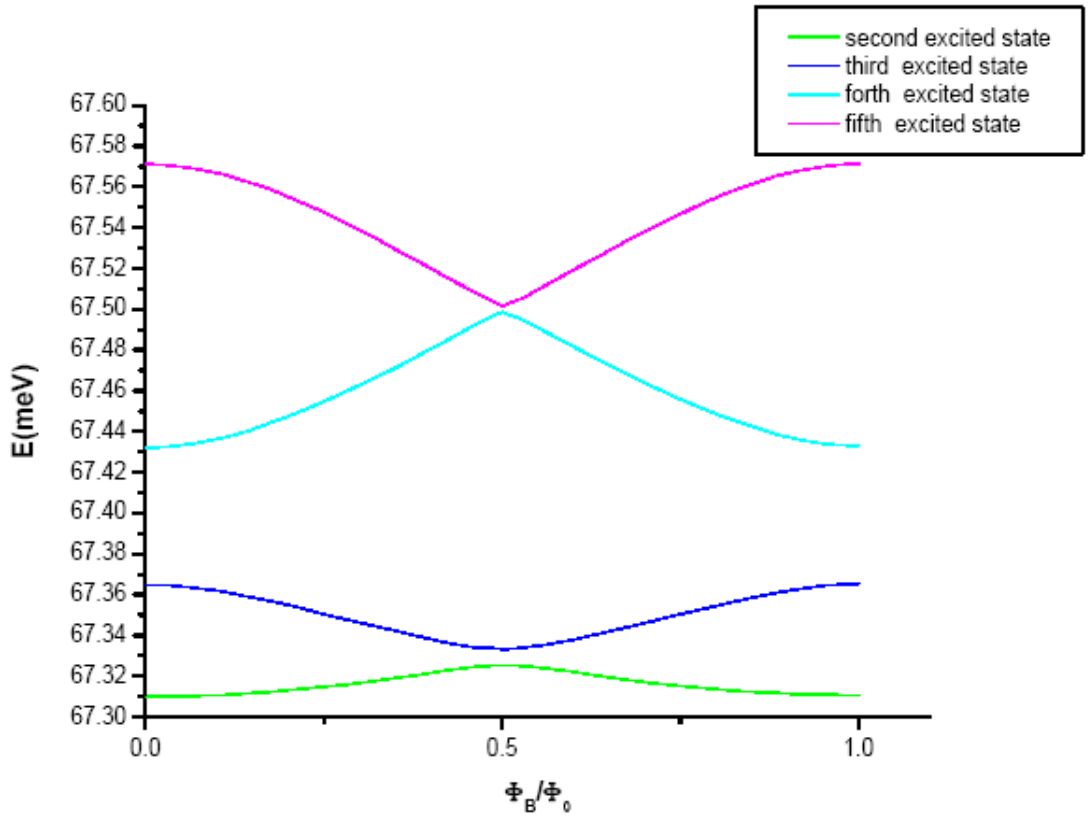

Figure 3.11: Energy spectra of a concentric quantum double ring with one impurity in the inner ring and the other in the outer ring.

3.4 Relation Between Φ_B and Aharonov-Bohm Effect

According to Eq.(3.3), AB effect appears whenever $\Phi_B = B\pi r^2$ is a positive multiple of Φ_0, i.e. $\frac{\Phi_B}{\Phi_0}$ is a positive integer. Because the magnetic flux quantum $\Phi_0 = \frac{hc}{e}$ is a constant, and is independent of the applied magnetic field and the area under magnetic field, so, when we enlarge the radius of the area under magnetic field, Therefore, to keep the Φ_B to be constant, the magnitude of the uniform magnetic field corresponds to the appearance of AB effect should be reduced when we enlarge the radius of the area under magnetic field.

We vary the radius of the magnetic flux area from $r = 80\ nm$ to $r = 150,\ 200,\ 300$, and $500\ nm$, and show the alternations of the periods of the AB oscillations in Fig.3.12 and Fig.3.13. As can be seen from Fig.3.12 and Fig.3.13, the period of the applied uniform magnetic field indeed becomes smaller when the radius of the area under the applied magnetic field becomes larger.

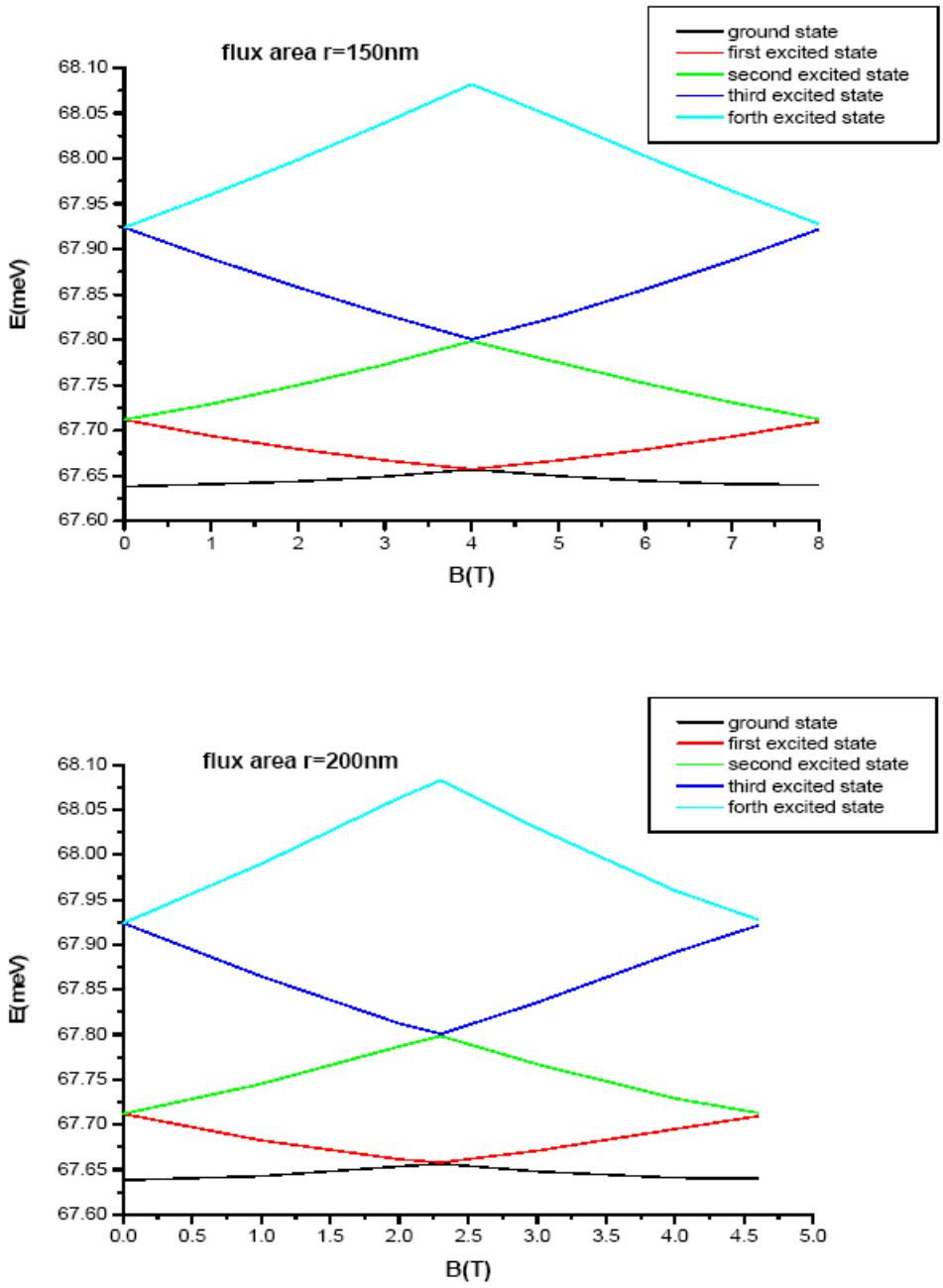

Figure 3.12: The energy spectra of a concentric quantum double ring for 150 nm (upper panel) and 200 nm (lower panel) wide of the flux-area radius.

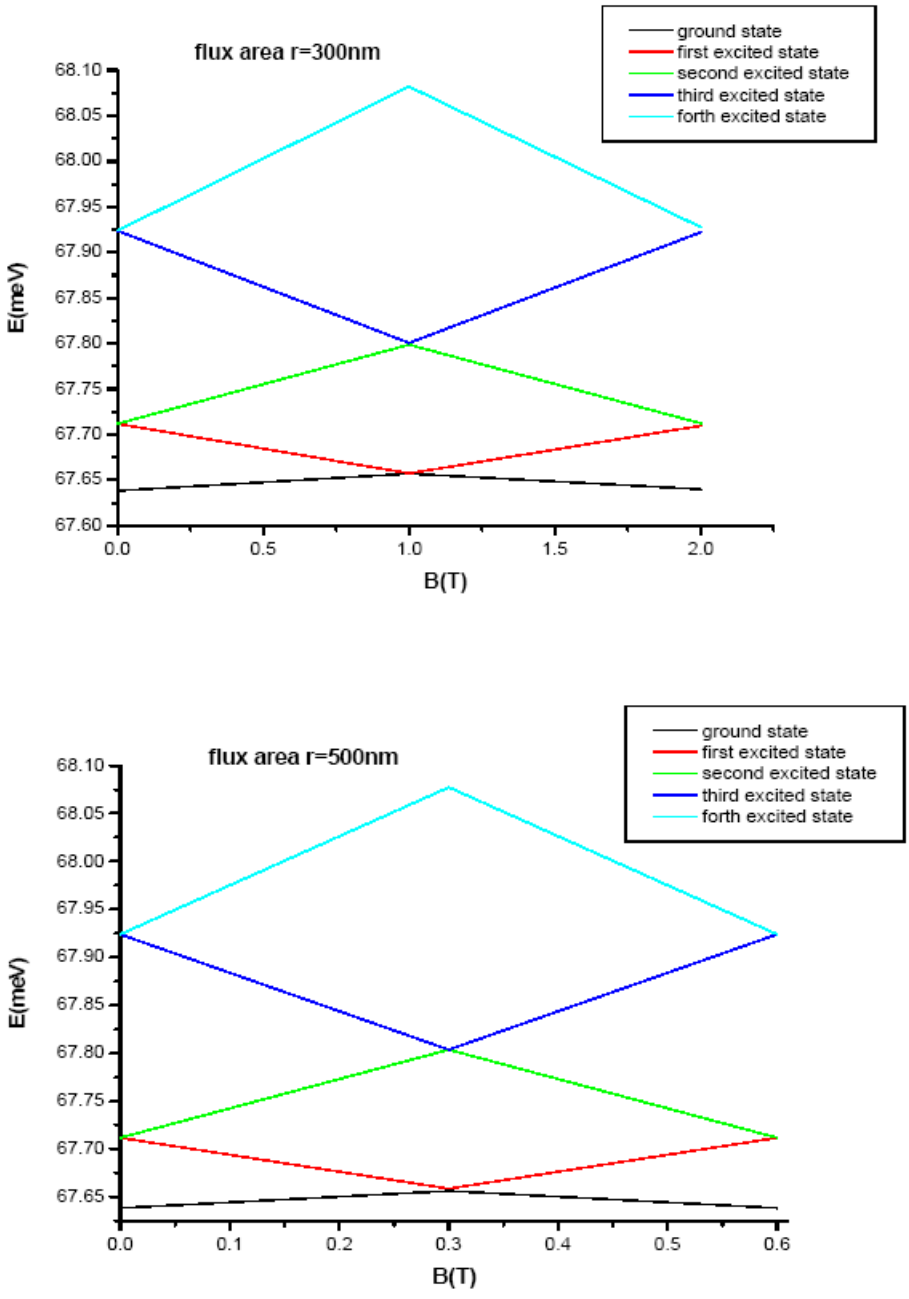

Figure 3.13: The energy spectra of a concentric quantum double ring for 300 nm (upper panel) and 500 nm (lower panel) wide of the flux-area radius.

Chapter 4

Conclusion

In this work, we employed the solutions of a free electron in a quantum ring to be a set of basis to solve the problem of a concentric quantum double ring with one finite potential barrier in the middle of the radial direction. The energy eigenvalues of the electron in the concentric quantum double ring with a uniform interior-threaded magnetic field are obtained by diagonalizing the Hamiltonian spanned by the basis. In addition, we also consider the problem of a concentric quantum double ring with single impurity located inside the inner ring. It is found that in the presence of the impurity the energy spectra have a gaps-like structure. If one further puts another identical impurity symmetric to the first impurity inside the inner ring, the gaps will disappear. But when one moves the second impurity to the outer ring, the gaps show up again due to the unsymmetrical radial part's wave functions. In the last section, we also find that due to the invariability of the universal magnetic flux quantum the periods of the magnitude of the applied uniform magnetic field became smaller when the magnetic flux area is enlarged.

Bibliography

[1] Y. Aharonov and D. Bohm, Phys. Rev. **115**, 485 (1959).

[2] R. A. Webb, S. Washburn, C. P. Umbach, and R. B. Laibowitz, Phys. Rev. Lett. **54**, 2696 (1985).

[3] Ho-Fai Cheung, Yuval Gefen, Eberhard K. Riedel, and Wei-Heng Shih, Phys. Rev. B **37**, 6050 (1988).

[4] A. Chaplik, Pis'ma Zh. *È*ksp. Teor. Fiz. **62**, 885 (1995) [JETP Lett. 62, 900 (1995)].

[5] R. A. Römer and M. E. Raikh, Phys. Rev. B **62**, 7045 (2000).

[6] A. Lorke and R. J. Luyken, Physica B **256-258**, 424 (1998); A. Lorke , R. J. Luyken, M. Fricke, J. P. Kotthaus, G. MedeirosRibeiro, J. M. Garcia, and P. M. Petroff, Microelectron. Eng. **47**, 95 (1999); H. Pettersson, R. p. J. Warburton, A. Lorke, K. Karrai, J. P. Kotthaus, J. M. Garcia, and P. M. Petroff, Physica E (Amsterdam) **6**, 510 (2000).

[7] A. Lorke, R. J. Luyken, A. O. Govorov, J. P. Kotthaus, J. M. Garcia, and P. M. Petroff, Phys. Rev. Lett. **84**, 2223 (2000).

[8] Jakyoung Song and Sergio E. Ulloa, Phys. Rev. B **63**, 125302 (2001).

[9] Hui Hu, Jia-Lin Zhu, Dai-Jun Li, and Jia-Jiong Xiong, Phys. Rev. B **63**, 195307 (2001).

[10] Jia-Lin Zhu, Xiquan Yu, and Zhensheng Dai, Phys. Rev. B **67**, 075404 (2003).

[11] Takaaki Mano, Takashi Kuroda, Stefano Sanguinetti, Tetsuyuki Ochiai, Takahiro Tateno, Jongsu Kim, Takeshi Noda, Mitsuo Kawabe, Kazuaki Sakoda, Giyuu Kido, and Nobuyuki Koguchi, Nano Lett. **5**, 425 (2005).

[12] J. J. Sakurai, p.136-137, Modern Quantum Mechanics.

[13] N. Byers and C. N. Yang, Phys. Rev. Lett. **7**, 46 (1961).

[14] D. S. Chuu, C. M. Hsiao, and W. N. Mei, Phys. Rev. B **46**, 3898 (1992).